Supplement of Earth Syst. Sci. Data, 18, 6859–6884, 2026
https://doi.org/10.5194/essd-18-6859-2026-supplement

Open Access Earth System Science Data

Supplement of

Signal-domain guided deep learning for gap-filling of XCO and XCH_4: a masked spatio-temporal fusion of TROPOMI and GEOS-Chem (2019–2023)

Chengkun An et al.

Correspondence to: Yuan Tian (ytian@ahu.edu.cn) and Youwen Sun (ywsun@ahu.edu.cn)

Supplementary tables

Table S1. Details of the TCCON sites used in this study, No. is the serial number.

No.	Site name	Latitude	Longitude	Location	Start date	End date
1	bremen01	53.104	8.85	Bremen, Germany	2009/1/6	2021/6/24
2	burgos01	18.5325	120.6496	Burgos, Philippines	2017/3/3	2023/6/23
3	darwin01	-12.425	130.891	Darwin, Australia	2013/1/1	2022/12/27
4	easttroutlake01	54.354	-104.987	East Trout Lake, Canada	2016/10/3	2024/2/15
5	edwards01	34.9599	-117.881	AFRC, Edwards, CA, USA	2013/7/20	2024/2/22
6	garmisch01	47.476	11.063	Garmisch, Germany	2007/7/18	2023/5/4
7	hefei01	31.91	117.17	Hefei, China	2015/11/2	2023/12/25
8	izana01	28.31	-16.5	Izana, Tenerife, Spain	2014/1/2	2023/8/30
9	karlsruhe01	49.103	8.44	Karlsruhe, Germany	2014/1/15	2023/6/26
10	lamont01	36.604	-97.486	Lamont, Oklahoma, USA	2011/4/16	2024/2/25
11	lauder03	-45.038	169.684	Lauder, New Zealand	2018/10/2	2023/12/28
12	nicosia01	35.141	33.381	Nicosia, Cyprus	2019/9/1	2023/5/10
13	orleans01	47.97	2.113	Orleans, France	2009/9/6	2023/6/23
14	parkfalls01	45.945	-90.273	Park Falls, Wisconsin, USA	2004/6/2	2024/2/25
15	pasadena01	34.136	-118.127	Pasadena, California, USA	2012/9/20	2024/2/25
16	reunion01	-20.901	55.485	Reunion Island, France	2015/3/1	2020/7/18
17	rikubetsu01	43.4567	143.7661	Rikubetsu, Hokkaido, Japan	2014/6/24	2021/6/30
18	sodankyla01	67.367	26.631	Sodankylä, Finland	2009/5/16	2023/5/30
19	tsukuba02	36.0513	140.1215	Tsukuba, Ibaraki, Japan, 125HR	2014/3/28	2021/3/31
20	wollongong01	-34.406	150.891	Wollongong, Australia	2013/1/4	2023/6/27
21	xianghe01	39.8	116.96	Xianghe, China	2018/6/14	2023/5/29

Table S2. Ablation study of site-based XCO validation using different reconstruction configurations. Metrics include coefficient of determination (R^2), root mean square error (RMSE, ppb), and mean bias (μ, ppb).

Configuration	R^2	RMSE	μ
DCT-only	0.8227	10.439	-3.815
DCT/SVD	0.8335	10.1166	-3.7682
DCT/SVD + residual CNN	0.8385	9.9619	-3.7677
DCT/SVD + residual U-Net	**0.845**	**9.7616**	**-3.686**
DCT/SVD + residual XGBoost	0.8392	9.9406	-3.7435

Table S3. Ablation study of site-based XCH_4 validation using different reconstruction configurations. Metrics include coefficient of determination (R^2), root mean square error (RMSE, ppb), and mean bias (μ, ppb).

Configuration	R^2	RMSE	μ
DCT-only	0.7056	17.5156	-6.9345
DCT/SVD	0.732	16.7111	-6.9635
DCT/SVD + residual CNN	0.7469	16.2404	-6.9162
DCT/SVD + residual U-Net	**0.7598**	**15.8212**	**-6.7858**
DCT/SVD + residual XGBoost	0.7476	16.2188	-6.9563

Table S4. (GEOS) Single-site validation results for GEOS-Chem, TROPOMI, and fused XCO data, with RMSE & μ in parts per billion (ppb).

SITE NAME	R^2			RMSE			μ		
	GEOS	TROPOMI	FUSION	GEOS	TROPOMI	FUSION	GEOS	TROPOMI	FUSION
burgos01	0.237	0.919	0.935	16.909	5.769	5.246	9.667	-2.799	-2.425
darwin01	-0.808	0.370	0.646	13.896	8.546	6.330	-9.241	-4.196	-2.848
easttroutlake01	-0.487	0.827	0.903	19.017	10.070	7.372	4.540	0.688	1.092
garmisch01	0.664	0.795	0.806	5.903	3.897	4.444	-1.453	0.737	1.113
hefei01	0.583	0.930	0.980	16.501	7.362	3.421	-15.897	-1.450	1.444
izana01	0.093	0.185	0.513	6.943	7.120	5.482	-3.692	5.790	3.909
karlsruhe01	0.521	0.411	0.596	7.055	6.892	6.441	4.002	-3.137	-4.337
lamont01	-0.134	0.534	0.580	9.297	6.447	6.013	5.209	-4.803	-3.650
lauder03	-0.524	0.849	0.663	11.990	3.893	5.666	-8.828	-2.228	-2.424
nicosia01	-0.251	0.868	0.847	8.114	2.791	3.008	5.978	0.557	-1.147
orleans01	0.581	0.791	0.537	6.704	6.656	8.947	3.012	-2.665	-2.786
parkfalls01	-0.468	0.899	0.811	19.445	6.597	8.677	7.525	-2.116	-2.106
reunion01	0.109	0.893	0.896	8.529	3.113	3.061	2.327	0.448	-0.859
rikubetsu01	0.635	0.961	0.899	7.674	2.893	4.545	1.122	0.064	0.438
sodankyla01	0.388	0.267	0.917	6.255	6.203	2.230	-0.775	2.807	1.381
tsukuba02	0.955	0.825	0.958	4.446	9.713	4.031	-2.817	-6.798	-1.684
wollongong01	-0.319	0.776	0.745	14.709	6.562	6.969	-5.625	-4.501	-4.418
xianghe01	0.279	0.269	0.553	11.965	10.749	9.469	-2.922	6.306	2.628

Table S5. (GEOS) Single-site validation results for GEOS-Chem, TROPOMI, and fused XCH_4 data, with RMSE & μ in parts per billion (ppb).

SITE NAME	R^2			RMSE			μ		
	GEOS	TROPOMI	FUSION	GEOS	TROPOMI	FUSION	GEOS	TROPOMI	FUSION
bremen01	-0.140	0.134	0.631	13.602	10.634	8.139	-0.024	-6.005	-2.375
burgos01	-0.280	0.741	0.877	24.716	13.217	8.892	-11.397	-7.712	-5.010
easttroutlake01	-0.560	0.371	0.322	27.858	18.152	20.471	-7.800	-10.457	-12.565
edwards01	-1.666	0.938	0.908	33.363	5.655	6.750	-20.863	2.314	4.679
garmisch01	-0.539	0.693	0.831	23.574	11.552	8.763	-4.177	-4.162	-3.266
hefei01	-1.130	0.882	0.770	38.129	8.789	12.575	-26.749	-3.298	-5.167
karlsruhe01	-1.466	0.546	0.561	31.590	13.937	14.156	-17.057	-8.526	-11.191
lamont01	-2.086	0.838	0.830	34.635	9.308	9.313	-22.403	-3.808	-4.785
lauder03	-1.178	0.725	0.742	33.162	12.366	12.116	-16.148	-7.392	-9.347
nicosia01	-2.566	0.670	0.893	32.223	10.568	5.954	-23.891	2.413	-1.740
orleans01	-1.780	0.551	0.705	30.640	13.366	11.070	-16.560	-6.472	-6.654
parkfalls01	-0.923	0.137	0.221	29.718	21.329	20.668	-12.079	-14.704	-16.099
pasadena01	-3.177	0.955	0.910	41.561	4.659	6.603	-32.970	-0.942	-3.476
rikubetsu01	0.230	0.740	0.715	15.539	9.189	9.892	6.588	-2.146	-4.784
tsukuba02	-0.582	0.777	0.712	15.420	6.238	7.147	-1.677	-2.308	-3.793
wollongong01	-1.396	0.195	0.347	29.981	19.964	17.320	-14.676	-12.975	-13.672
xianghe01	0.033	0.855	0.888	25.528	10.349	9.120	-9.444	-0.354	-1.247

Table S6. Validation statistics of XCO under different TROPOMI missing-rate intervals. GEOS-Chem results were bias-corrected before validation, and RMSE and μ are reported in parts per billion (ppb).

MR	R^2			RMSE			μ		
	GEOS	TROPOMI	FUSION	GEOS	TROPOMI	FUSION	GEOS	TROPOMI	FUSION
$MR < 0.3$	0.65	0.97	0.94	16.60	2.04	5.69	-0.22	-0.43	-1.10
$0.3 \leq MR \leq 0.5$	0.63	0.96	0.93	13.44	2.96	5.16	0.02	-0.88	-1.21
$MR > 0.5$	0.48	0.89	0.91	11.99	6.16	5.65	0.79	-0.87	-1.40

Table S7. Validation statistics of XCH_4 under different TROPOMI missing-rate intervals.GEOS-Chem results were bias-corrected before validation, and RMSE and μ are reported in parts per billion (ppb).

MR	R^2			RMSE			μ		
	GEOS	TROPOMI	FUSION	GEOS	TROPOMI	FUSION	GEOS	TROPOMI	FUSION
$MR < 0.3$	-0.15	0.95	0.87	29.10	3.05	9.66	-2.87	-0.57	-4.37
$0.3 \leq MR \leq 0.5$	-0.17	0.94	0.85	28.39	3.84	10.78	-3.19	-0.65	-2.17
$MR > 0.5$	0.34	0.81	0.83	29.84	15.84	15.40	-0.80	-5.48	-7.30

Table S8. Sensitivity of the 2019 daily XCO reconstruction to the SVD cumulative-energy threshold.

SVD energy threshold (%)	Spatial R vs. 80%	RMSE vs. 80% (ppb)	μ vs. 80% (ppb)	SD ratio vs. 80%	Hotspot overlap
70	0.99998	0.206	-0.088	0.99989	0.983
75	0.99999	0.160	-0.086	0.99990	0.984
80	1.00000	0.000	0.000	1.00000	1.000
85	0.99996	0.271	0.000	1.00000	1.000
90	0.99992	0.382	0.003	0.99965	0.999
95	0.99984	0.616	0.285	1.00019	0.975

Note: The 80% threshold was used as the reference case. Spatial R denotes the Pearson correlation coefficient calculated across valid grid cells between each threshold experiment and the 80% case. RMSE, μ, and SD ratio were also calculated relative to the 80% case, where SD denotes the spatial standard deviation. Hotspot overlap was calculated using the upper 10% of reconstructed XCO grid cells. All statistics were derived from the 2019 global daily 0.25° × 0.25° CO reconstruction experiments.

Table S9. Seasonally adjusted short-term rates of change and 95% confidence intervals for XCO over rice-growing regions during 2019–2023. Unit: ppb/year.

Region	Rate of change		95% confidence interval	
	TROPOMI	Fusion	TROPOMI	Fusion
Northeast China	−2.36	−2.28	−3.30 to −1.43	−3.30 to −1.27
Southeast China	−1.29	−1.76	−2.15 to −0.43	−2.79 to −0.72

Table S10. Seasonally adjusted short-term rates of change and 95% confidence intervals for XCH_4 over rice-growing regions during 2019–2023. Unit: ppb/year.

Region	Rate of change		95% confidence interval	
	TROPOMI	Fusion	TROPOMI	Fusion
Northeast China	12.08	12.16	11.24 to 12.92	11.27 to 13.04
Southeast China	12.16	11.78	10.83 to 13.49	9.72 to 13.83

Table S11. Overall statistics of the TROPOMI CO averaging-kernel sensitivity test in 2019, with RMSE and μ in parts per billion (ppb).

Comparison	R^2	RMSE	μ
Original GEOS-Chem vs. TROPOMI	0.543	28.17	-17.09
AK-smoothed GEOS-Chem vs. TROPOMI	0.565	28.66	-18.34

Supplementary figures

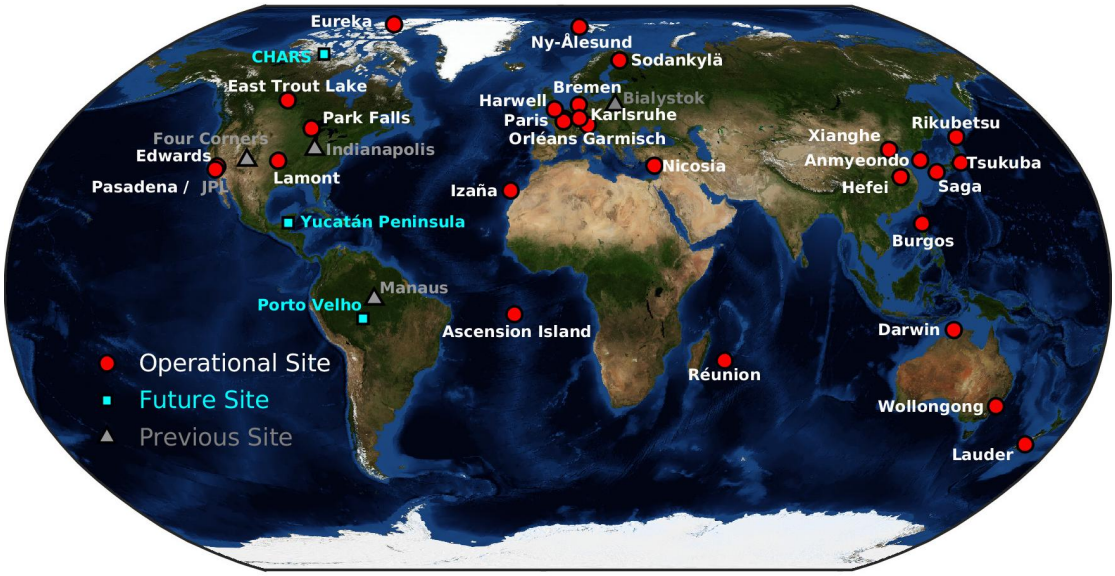

Figure S1. Global distribution of TCCON sites, including operational sites, future sites, and previous sites, respectively.

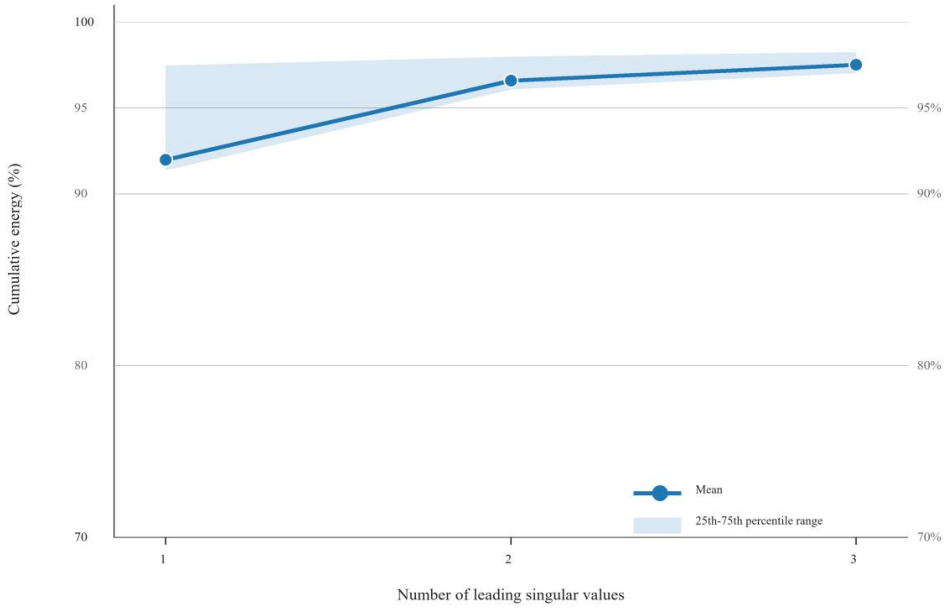

Figure S2. Cumulative singular-value energy explained by the leading singular values in the 2019 daily global XCO reconstruction.

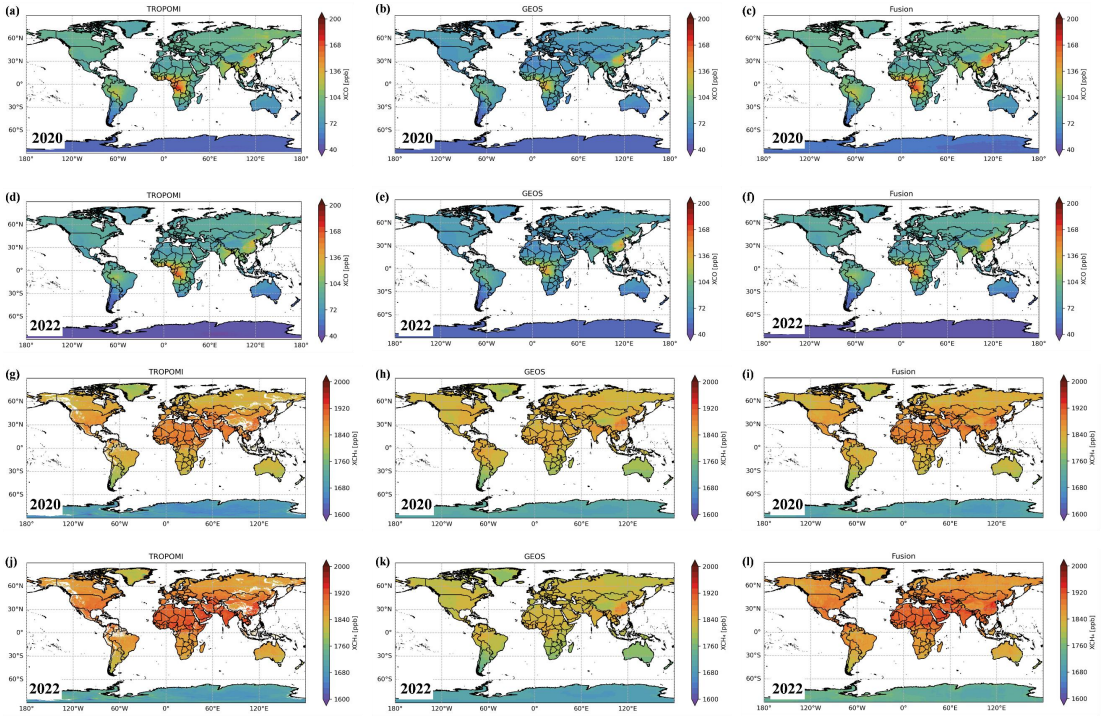

Figure S3. Annual mean global concentration distributions of XCO from (a, d) TROPOMI, (b, e) GEOS-Chem, and (c, f) fused data, and XCH_4 from (g, j) TROPOMI, (h, k) GEOS-Chem, and (i, l) fused data. Color bars indicate XCO and XCH_4 concentrations in parts per billion.

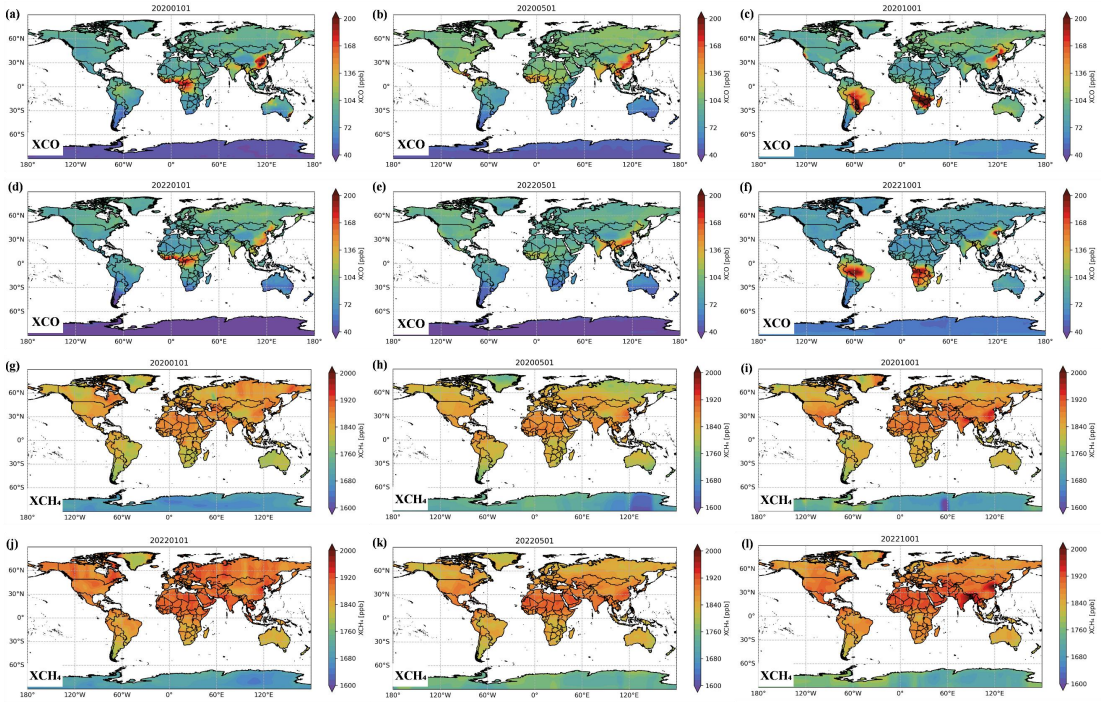

Figure S4. Single-day global concentration distributions of fused (a–f) XCO and (g–l) XCH_4 data. Color bars indicate XCO and XCH_4 concentrations in parts per billion.

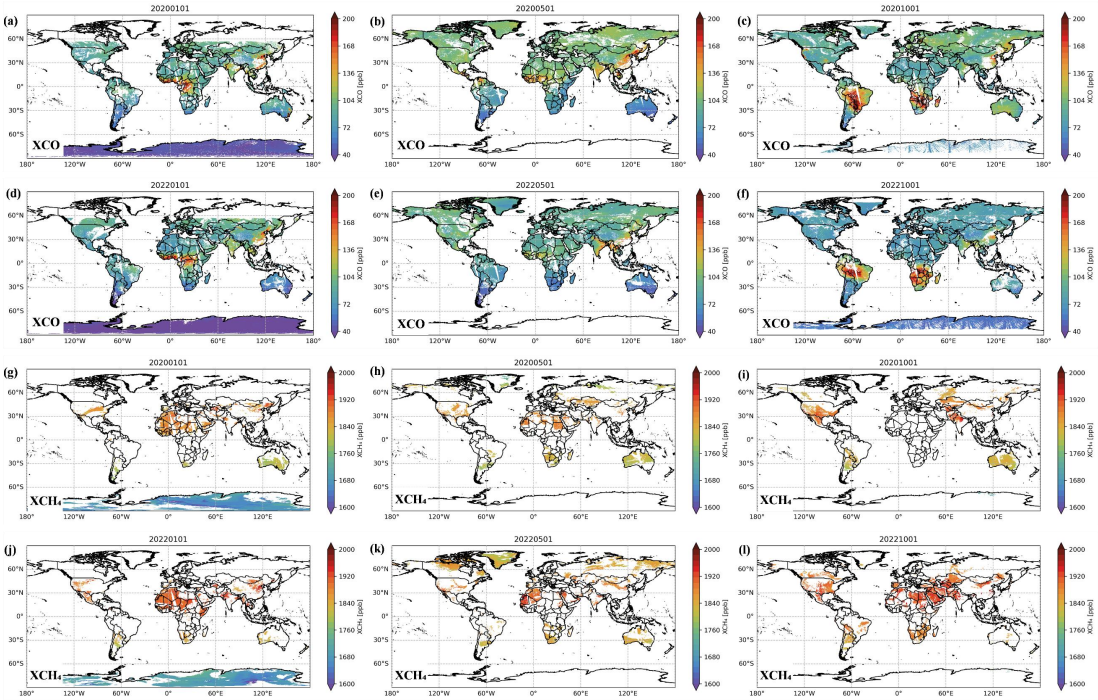

Figure S5. Single-day global concentration distributions of (a–f) XCO and (g–l) XCH_4 observed by TROPOMI. Color bars indicate XCO and XCH_4 concentrations in parts per billion.

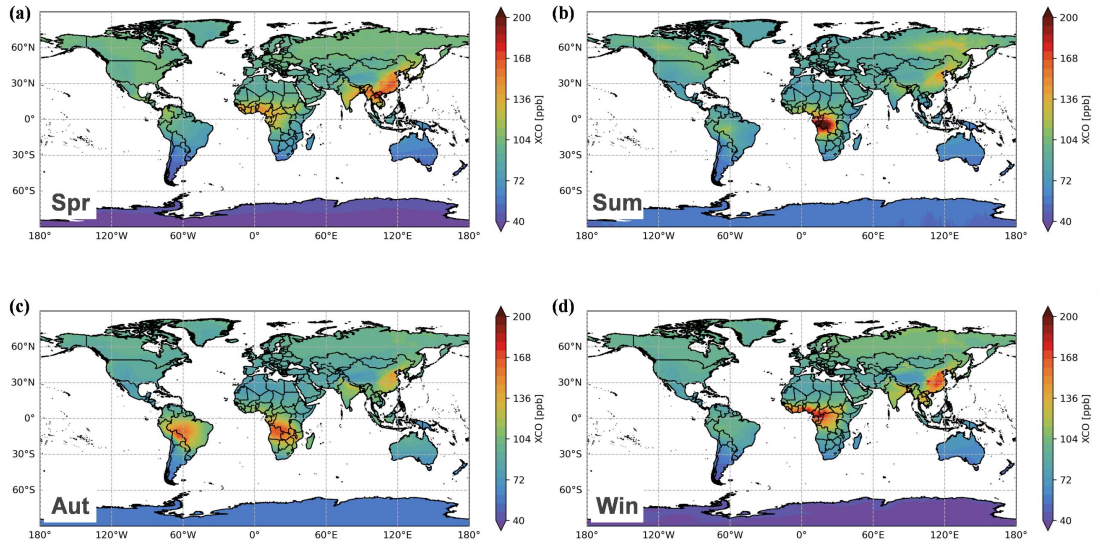

Figure S6. Seasonal fusion data of XCO from 2019 to 2023 in global concentration distribution. Color bars indicate XCO concentrations in parts per billion. (a) Spr, (b) Sum, (c) Aut and (d) Win represent December through February, March through May, June through August, and September through November, respectively.

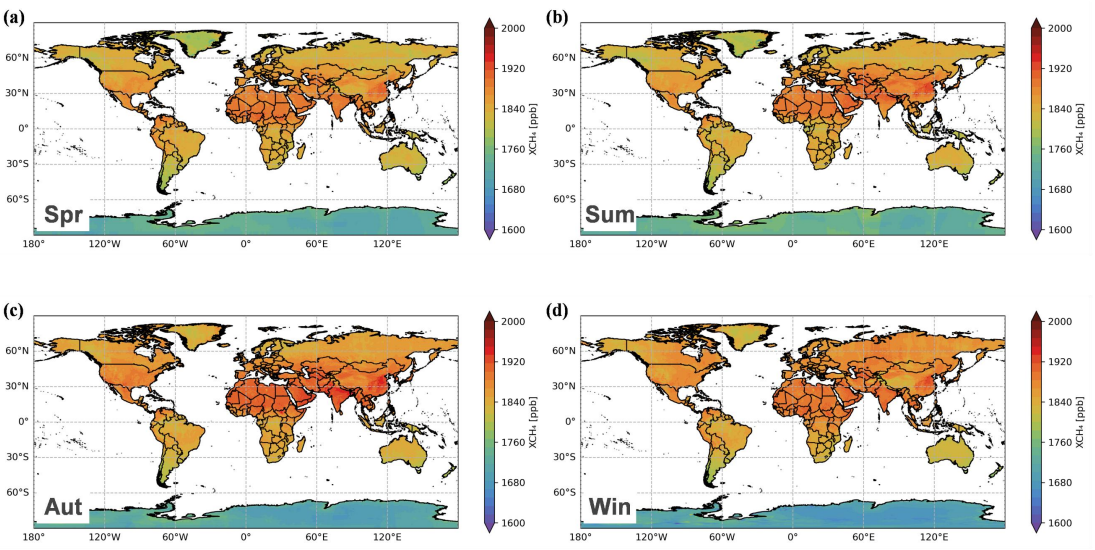

Figure S7. Seasonal fusion data of XCH_4 from 2019 to 2023 in global concentration distribution. Color bars indicate XCH_4 concentrations in parts per billion. (a) Spr, (b) Sum, (c) Aut and (d) Win represent December through February, March through May, June through August, and September through November, respectively.

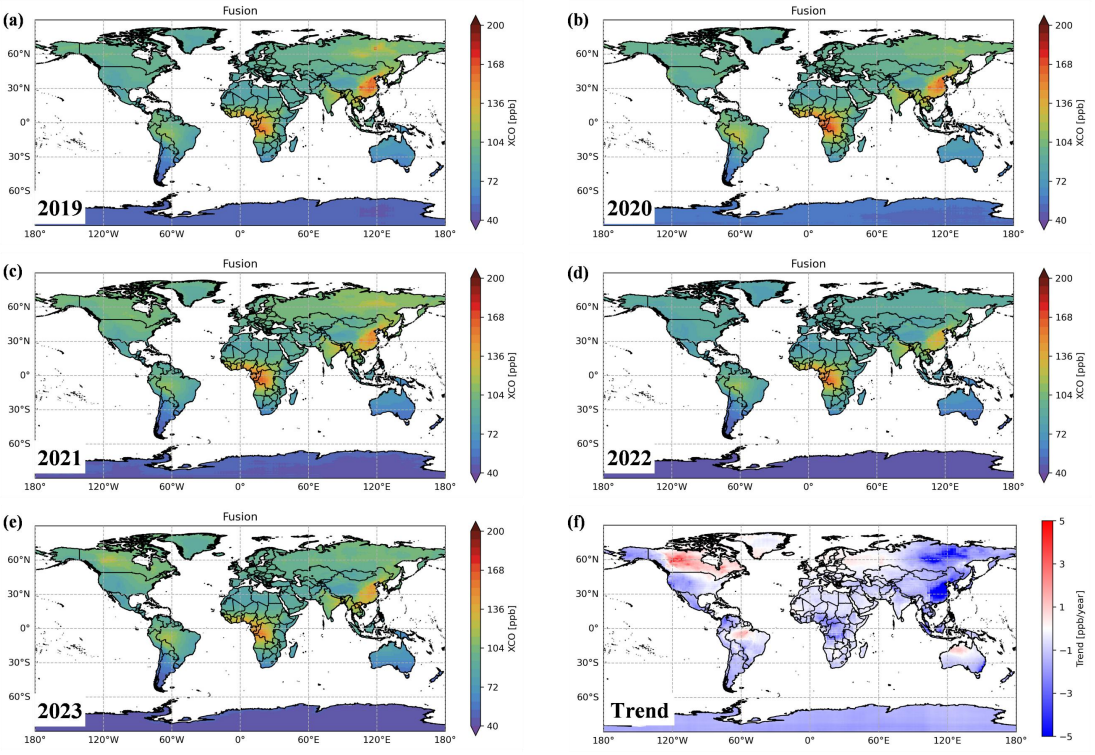

Figure S8. Annual mean global concentration distributions of fused XCO data from 2019 to 2023. Color bars indicate XCO concentrations in parts per billion. (a–e) Annual mean XCO concentrations; (f) annual rate of change in XCO, in parts per billion per year.

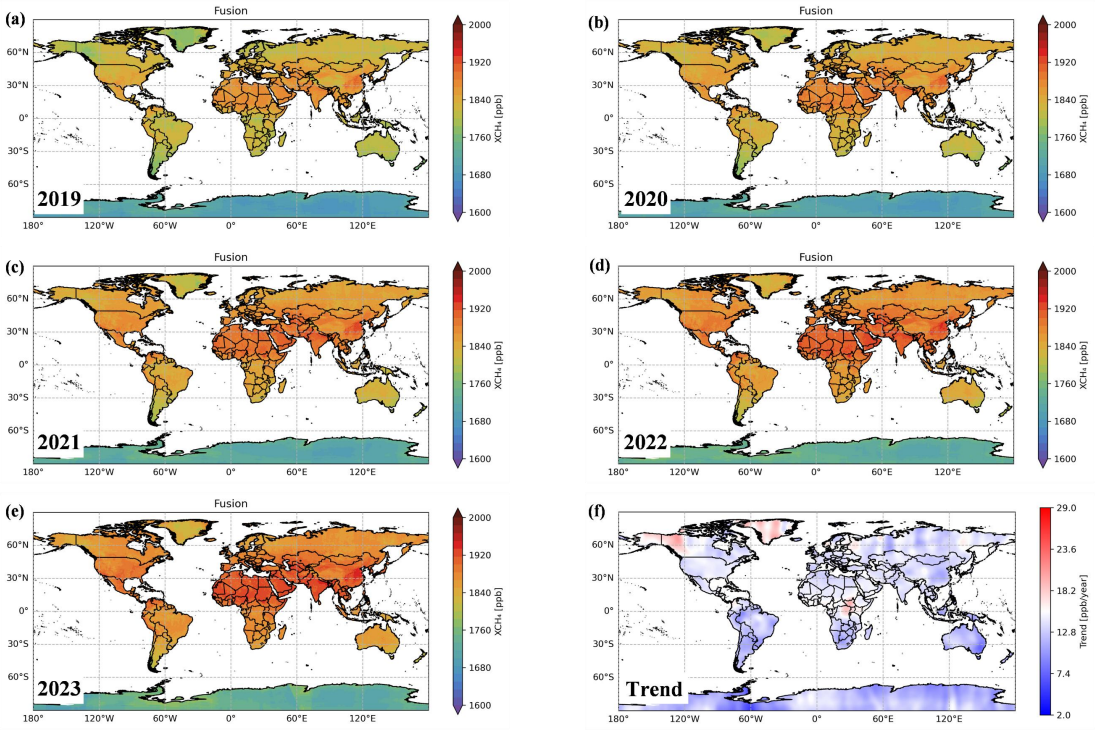

Figure S9. Annual mean global concentration distributions of fused XCH_4 data from 2019 to 2023. Color bars indicate XCH_4 concentrations in parts per billion. (a–e) Annual mean XCH_4 concentrations; (f) annual rate of change in XCH_4, in parts per billion per year.

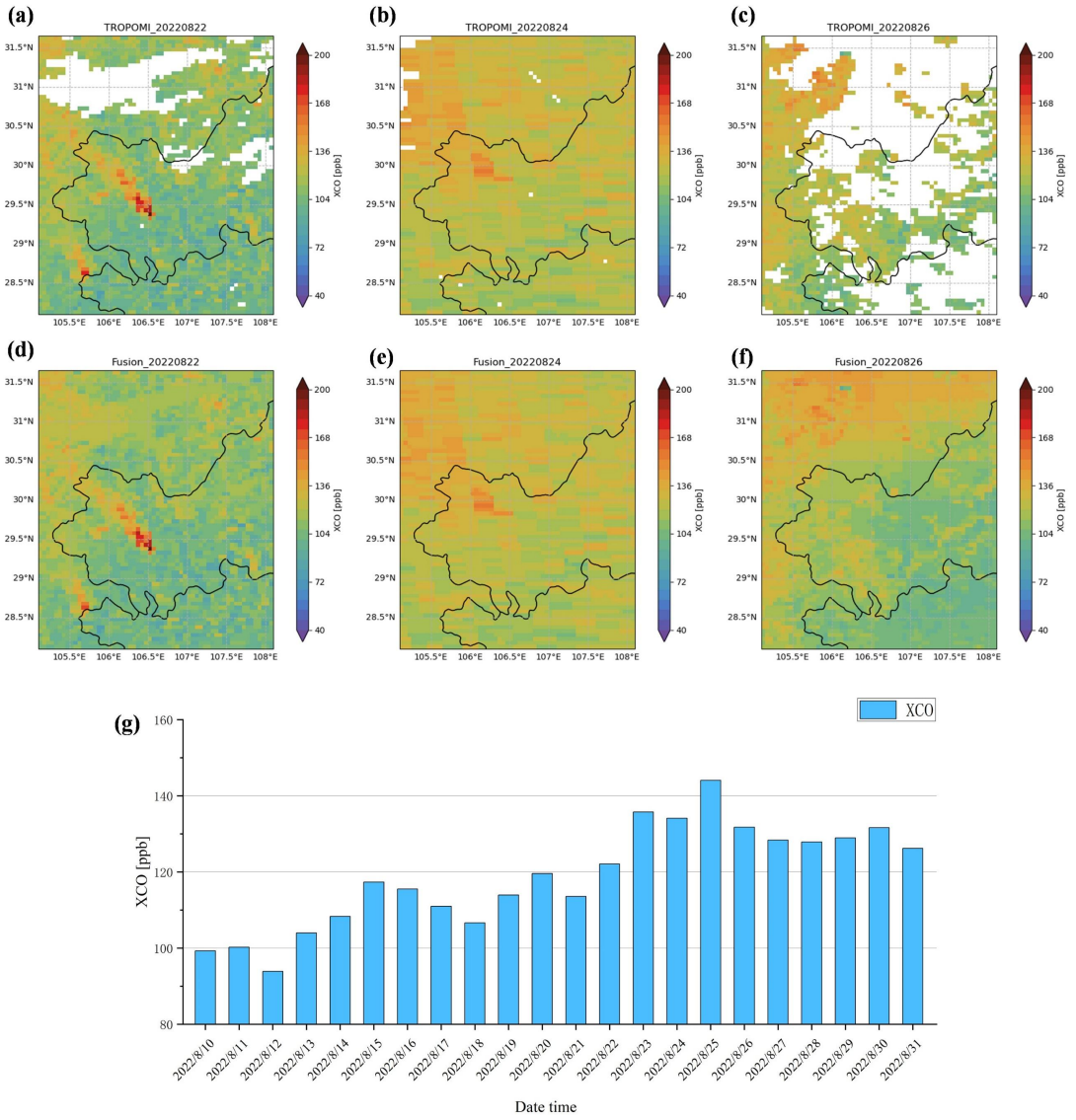

Figure S10. Single-day XCO concentration distributions over the Chongqing region from (a–c) TROPOMI and (d–f) fused data. Color bars indicate XCO concentrations in parts per billion. (g) Histogram of daily fused XCO concentration changes in mid- to late-August 2022, in parts per billion.

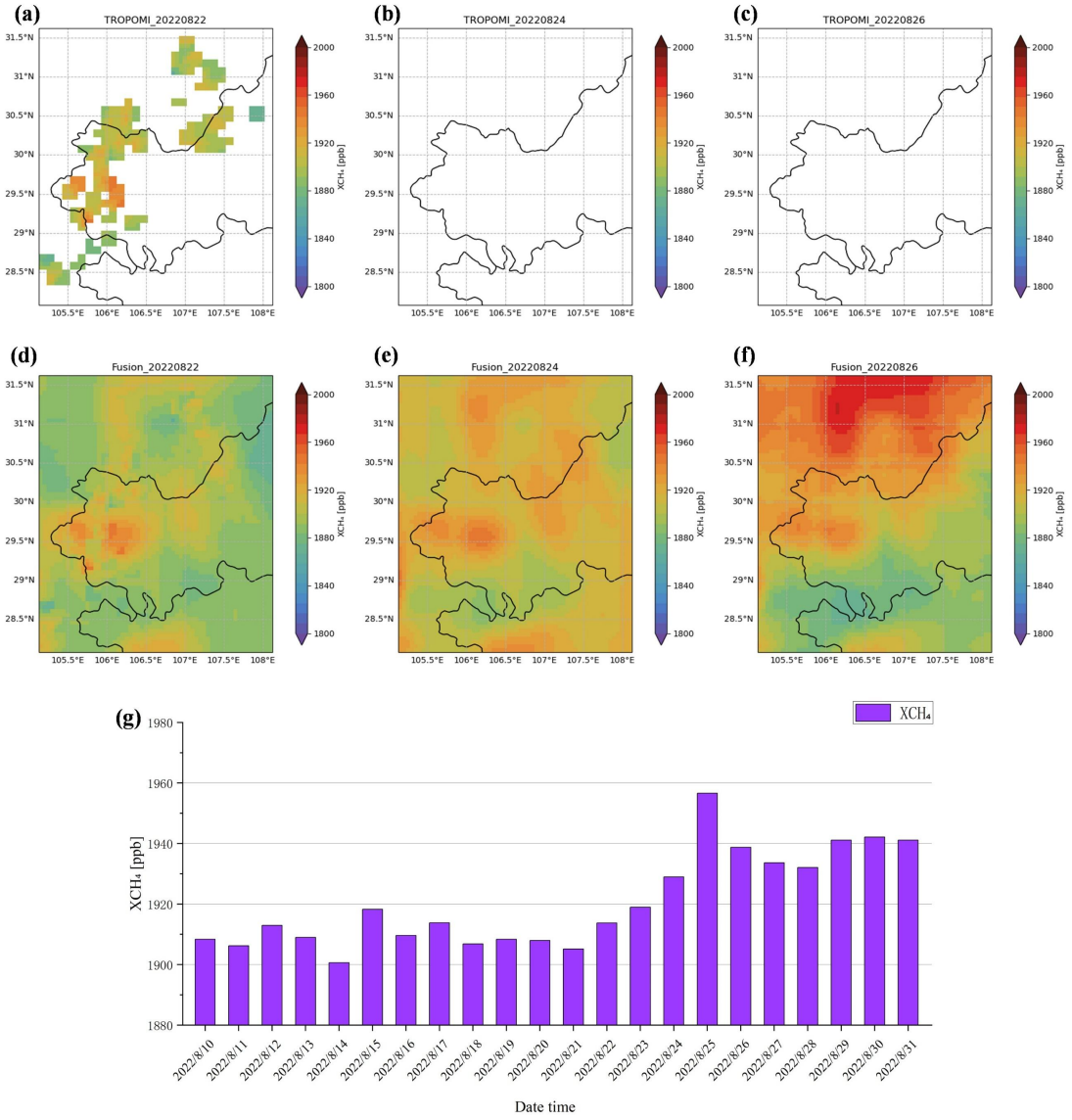

Figure S11. Single-day XCH_4 concentration distributions over the Chongqing region from (a–c) TROPOMI and (d–f) fused data. Color bars indicate XCH_4 concentrations in parts per billion. (g) Histogram of daily fused XCH_4 concentration changes in mid- to late-August 2022, in parts per billion.

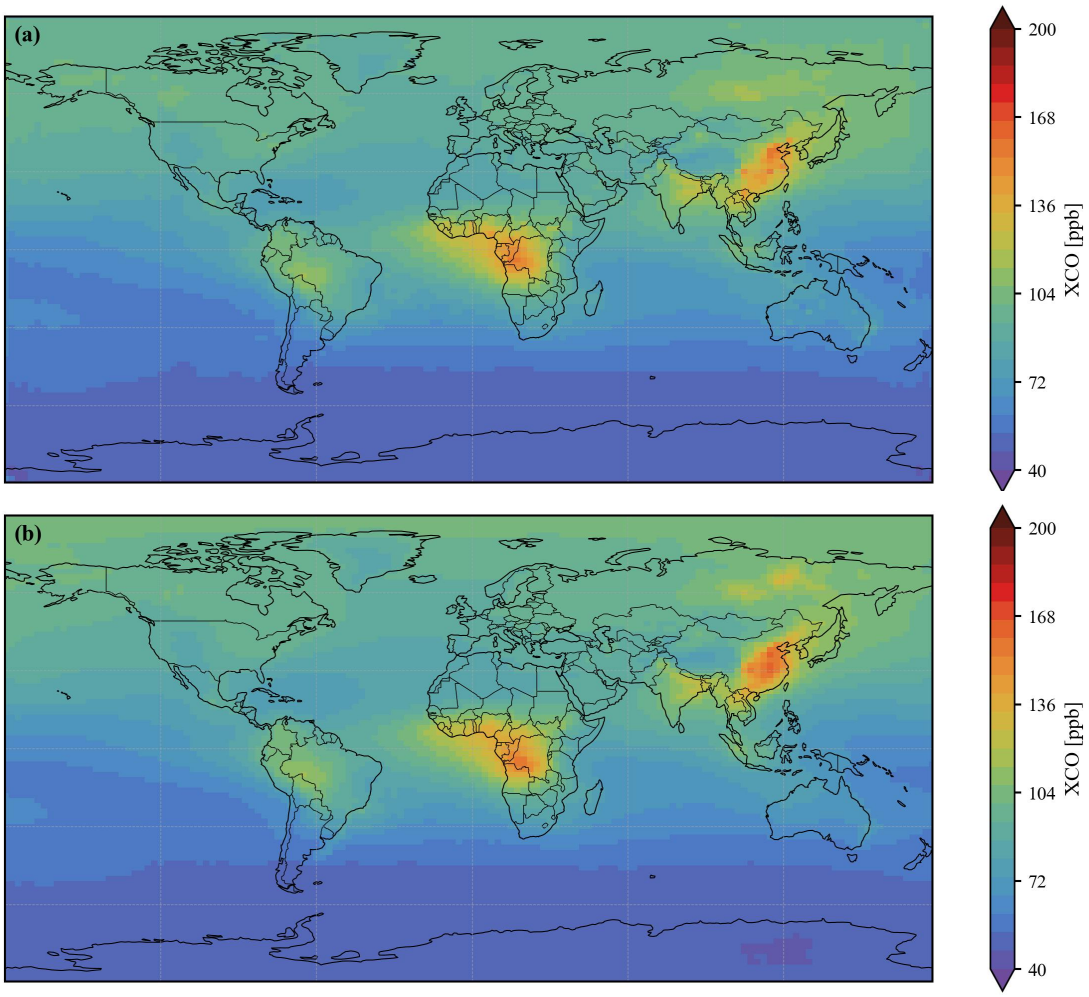

136 **Figure S12.** Spatial comparison of the 2019 XCO resolution-sensitivity experiment. (a) Fused XCO
137 data generated directly at the native 2° × 2.5° GEOS-Chem resolution. (b) Fused XCO data obtained
138 by aggregating the 0.25° resolution fused XCO data to the same 2° × 2.5° grid using the area-
139 weighted averaging method.

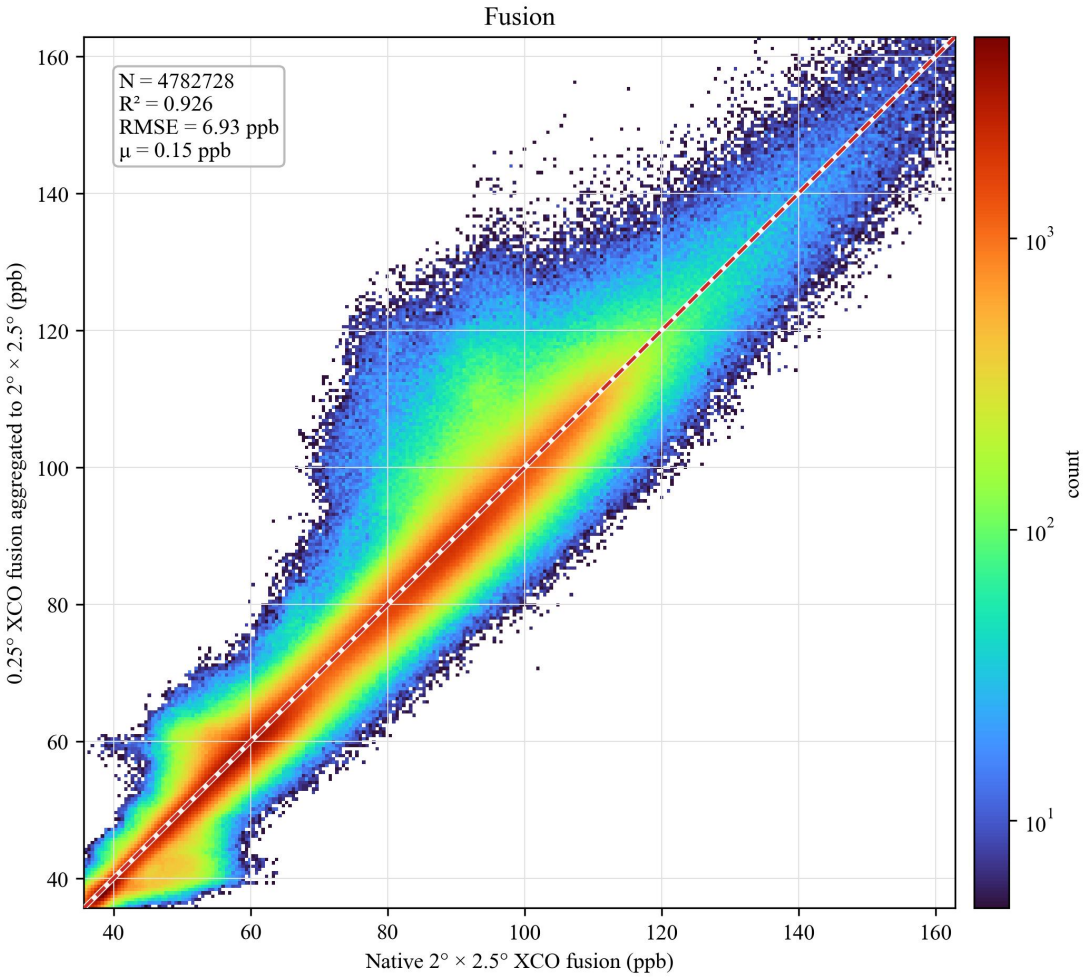

Figure S13. Quantitative comparison of the 2019 XCO resolution-sensitivity experiment.